T Cell Cross-Reactivity and Conformational Changes during TCR Engagement

Jean K. Lee,[1,4] Guillaume Stewart-Jones,[2] Tao Dong,[1] Karl Harlos,[2] Kati Di Gleria,[1] Lucy Dorrell,[1] Daniel C. Douek,[4] P. Anton van der Merwe,[3] E. Yvonne Jones,[2] and Andrew J. McMichael[1]

[1]*Human Immunology Unit, Medical Research Council, Weatherall Institute of Molecular Medicine, John Radcliffe Hospital, Oxford OX3 9DS, England, UK*
[2]*Division of Structural Biology, Wellcome Trust Centre for Human Genetics, Oxford OX3 7BN, England, UK*
[3]*Sir William Dunn School of Pathology, University of Oxford, Oxford OX1 3RE, England, UK*
[4]*Human Immunology Section, Vaccine Research Center, National Institute of Allergy and Infectious Diseases, National Institutes of Health, Bethesda, MD 20892*

Abstract

All thymically selected T cells are inherently cross-reactive, yet many data indicate a fine specificity in antigen recognition, which enables virus escape from immune control by mutation in infections such as the human immunodeficiency virus (HIV). To address this paradox, we analyzed the fine specificity of T cells recognizing a human histocompatibility leukocyte antigen (HLA)-A2–restricted, strongly immunodominant, HIV gag epitope (SLFNTVATL). The majority of 171 variant peptides tested bound HLA-A2, but only one third were recognized. Surprisingly, one recognized variant (SLYNTVATL) showed marked differences in structure when bound to HLA-A2. T cell receptor (TCR) recognition of variants of these two peptides implied that they adopted the same conformation in the TCR–peptide–major histocompatibility complex (MHC) complex. However, the on-rate kinetics of TCR binding were identical, implying that conformational changes at the TCR–peptide–MHC binding interface occur after an initial permissive antigen contact. These findings have implications for the rational design of vaccines targeting viruses with unstable genomes.

Key words: HIV • CTL • HLA-A2 • binding conformation • fine specificity

Introduction

Current information on the extent of T cell cross-reactivity presents a paradox; there is evidence that T cells are broadly cross-reactive (1–4), but other data show narrow specificities (5–11). The balance achieved between these opposing characteristics is particularly pertinent to antiviral immunity, where antigenic variation may result in poor T cell recognition and profoundly affect the outcome of an infection (12). Although there are clear examples of virus escape from T cell immune responses by point mutations in key epitopes (13–18), it is possible that such escape is the exception, as most of the examples involve escape by a subset of peptide variants that fail to bind to the presenting HLA molecule. As T cells that cross-react to more than one subtype of a virus such as HIV have been described previously (19–23), there is intense debate about whether to match HIV vaccines and virus sequences (24, 25).

Cross-reactivity is a characteristic of T cell recognition because all T cells that reach the periphery must have bound previously to at least one combination of self-peptide and major histocompatibility complex molecule to have been positively selected in the thymus (1, 2). Furthermore, there are examples of mature T cells capable of cross-reacting with different peptide–MHC complexes; i.e., Epstein Barr virus EBNA3-HLA-B8–specific cytotoxic T cells that cross-react with various self peptides presented by HLA-B35 (3). Examples are also known for MHC class II–restricted $CD4^+$ T cells and such cross-reactivity may underlie autoimmune disease (4). In contrast, fine specificity studies of T cell

The online version of this article contains supplemental material.

Address correspondence to Andrew J. McMichael, Human Immunology Unit, Medical Research Council, Weatherall Institute of Molecular Medicine, John Radcliffe Hospital, Oxford OX3 9DS, England, UK. Phone: 44-1865-222336; Fax: 44-1865-222600; email: andrew.mcmichael@ndm.ox.ac.uk

Abbreviations used in this paper: pMHC, peptide-MHC; SFU, spot-forming units.

clones, in functional assays, have shown great sensitivity to epitope variation. In some cases, the antigens were closely related to self (5–7), so tolerance to the self epitopes might have preselected T cells that react to only very limited epitope variants. Similarly, T cells responding to peptide immunogens (8) could show restricted specificity because the antigen is suboptimal. However, three studies of human $CD8^+$ T cell responses to natural viral antigens (9–11) show that immunodominant $CD8^+$ T cells are finely restricted in epitope specificity.

To assess systematically the extent of cross-reactivity in clinically relevant $CD8^+$ T cells, we focused on the response to a highly immunodominant HLA-A2–restricted and naturally highly variable epitope, SLFNTVATL, in HIV gag p17. We explored sensitivity of this T cell response to immune escape by single amino acid change. As >40% of the population express HLA-A2, the sensitivity of this dominant T cell response to HIV variation could have a significant impact on the control of HIV infection.

We show that most single amino acid changes, when applied to this peptide sequence, abolish functional recognition for both specific T cell clones and for uncloned T cell responses in the blood of different HIV-infected patients. Although many altered peptides were not recognized, the T cells reacted to both of the common A and B subtype virus variants, which differ at position three, phenyalanine (SLFNTVATL) and tyrosine (SLYNTVATL), respectively; cross-reactivity to these two variants is typical of ~50% of T cell responses in the population (26). However, when we determined the crystal structures of HLA-A2 with the SLFNTVATL and SLYNTVATL peptides, we found a striking structural difference, resulting from a significant change in the conformation of the bound peptide. The ability of T cells to cross-react despite this large difference appeared incompatible with the observed sensitivity of the T cell recognition to other very small changes in sequence, which would typically equate to relatively small chemical or steric differences at the TCR binding surface. We showed that the T cells show similar patterns of recognition of further single amino acid variants of these two peptides. In combination, these data suggest that, ultimately, the T cells recognize a conformation common to both peptides and, therefore, that one or both change conformation on TCR binding. Kinetic and thermodynamic studies of TCR interaction with these two peptide–HLA-A2 molecules imply that the conformational change required for the TCR and the peptide-MHC (pMHC) to dock in a stable complex probably occurs after the initial phase of TCR binding. Thus, first contact between TCR and pMHC may tolerate marked variation in peptide structure and sequence, but once any energetically favorable conformational adjustments have been generated, the functional TCR interaction is very specific, requiring a high level of conservation in the detailed features of the pMHC.

Materials and Methods

Cell Culture. HLA-A2–restricted, HIV-1–specific CTLs were cloned by limiting dilution of PBMCs of infected donors. Clones recognized both subtypes A and B of the HLA-A2–restricted gag p17 epitope, SLFNTVATL and SLYNTVATL, respectively.

Peptides. Single amino acid variants of SLFNTVATL, an HLA-A2–restricted epitope from the HIV p17 gag matrix protein, were synthesized using the Advanced Chemtech automated synthesizer. Peptides were checked for purity by HPLC. Most peptides (156 out of 171) showed >95% purity.

ELISPOT Assay. ELISPOT plates (Millipore) were coated with anti–human IFN-γ Ab (Mabtech) for 2 h at 37°C. The plates were washed six times with PBS 0.05% Tween and incubated for 1 h with R10 at room temperature. 50 μl HLA-A2 B cells at 10^5 cells/ml were added to each well in duplicate. Before adding to wells, B cells were prepulsed with each variant peptide at 2 μM final concentration for 20 min at 37°C. Next, 50 μl CTL clones at 4×10^3 cells/ml were added to a final volume of 100 μl. The plates were incubated overnight at 37°C. After cell removal, a second biotinylated Ab to human IFN-γ was added and incubated at room temperature for 2 h. After washing, the plates were developed with streptavidin–alkaline phosphatase (Mabtech) and colorimetric substrate. Spot-forming units (SFU) were counted using an automated ELISPOT reader. Background counts for negative control wells without peptides were always <5 spots/well. Results were expressed as percentage of SFU compared with the index peptide (SLFNTVATL).

Cytotoxicity Assay. EBV-transformed HLA-A201 B cells were labeled with ^{51}Cr and resuspended to 10^5 cells/ml. 50 μl were transferred to each well of a 96-well plate containing 16.7 μl of peptide diluted in RPMI 1640. Variant peptides were initially tested at concentrations of 10, 2, 1, 0.1, 0.01, and 0.001 μM. After 30 min at 37°C, CTL clones were added in 100 μl R10 to give an E/T ratio of 5:1. The plates were incubated at 37°C for 5 h. 30 μl of the supernatant was collected, and 150 μl of scintillator fluid was added to each well. ^{51}Cr release was counted in duplicate using a Microbeta counting program. Spontaneous release was <25% of detergent release. Percent specific lysis was calculated as the following: 100 × [(experimental release − spontaneous release) / (detergent release − spontaneous release)]. Results were expressed as percent of lysis seen with the SLFNTVATL peptide.

TCR Sequencing and Cloning. RNA was extracted using Tri-Reagent from CTL clones and subjected to an RT-PCR amplification technique with a switching mechanism at the 5′ end of the RNA transcripts (27). This was performed with C-region α primer: TCRAC, 5′-GTCCATAGACCTCATGTCTAGCACAG-3′; and a C-region β primer: TCRBC, 5′-ATTCACCCACCAGCTCAGCTCCACG-3′. Sequencing was performed with gel-purified PCR products using the dideoxy chain-termination method on a Megabase 1000. Specific primers were designed to clone the G10 and T5-004 TCR α and β chains into the *Escherichia coli* expression vector Pett22b$^+$ (Novagen) without the native leader peptide sequences, and the α chain was cloned in frame with the COOH-terminal vector His_6 tag. Residues α threonine 166 and β threonine 174 were mutated to cysteines.

Clonotype Analysis. PBMCs were stained with PE-conjugated SLFNTVATL– or SLYNTVATL–HLA-A2 tetramers, and fluorochrome-conjugated antibodies specific for CD3 and CD8. Tetramer$^+$ $CD8^+$ T cells (3,000 cells each) were sorted using a FACSDiVA (Becton Dickinson) directly into collection tubes containing 100 μl RNAlater (Ambion). mRNA was extracted and template switch-anchored RT-PCR was performed using a TCRBC primer to obtain full-length TCRBVDJ PCR products as described previously (28). PCR products were ligated into the pGEMT Easy Vector (Promega) and used to transform compe-

tent bacteria. Colonies were selected, amplified by PCR with standard M13 primers, and sequenced as described previously (28). Sequences were analyzed using Sequencher.

Protein Expression, Refolding, and Purification. Residues 1–278 of the HLA-A2 heavy chain, cloned in Pett22b$^+$, were expressed in BLR (Novagen) *E. coli* as inclusion bodies, refolded, and purified with the HIV-1 p17 peptides SLFNTVATL or SLYNTVATL and β-2 microglobulin as described previously (29). For soluble G10 TCR production, residues 1–211 and 1–242 from the α and β chains, respectively, were cloned into Pett22b$^+$ (Novagen), and the protein was expressed in BLR strain *E. coli* (Novagen) as inclusion bodies. Soluble TCR protein was refolded and purified as described previously (30). Soluble G10 TCR was diluted to 0.106, 0.313, 0.625, 1.25, 2.5, 5, 10, 20, 40, and 80 μM in HBS buffer (Biacore) for the surface plasmon resonance experiment.

Crystallization and Data Collection. All crystallizations were performed using the hanging drop vapor diffusion technique. Single HLA-A2–SLFNTVATL or HLA-A2–SLYNTVATL crystals grew at 4°C at a final concentration of 10 mg/ml in 14% PEG 6000 50 mM MES, pH 6.5, to dimensions of ~150 μm × 80 μm × 40 μm. Crystals were harvested and soaked briefly and sequentially in reservoir solutions containing 10 and 20% glycerol, flash cooled, and maintained at 100 K in a cryostream (Oxford Cryosystems). Two high resolution datasets were collected at station 14.2 of the Synchrotron Radiation Source using an ADSC-q4 (Area Detector Systems Corporation) charged-coupled device detector. The crystals belonged to space group P1, and datasets were auto-indexed and integrated with the program DENZO (31), followed by scaling with the program SCALEPACK (31); the results are summarized in Table I.

Structure Determination, Refinement, and Analysis. Crystal structures were determined by molecular replacement using the program EPMR (32). For the HLA-A2–SLFNTVATL and the HLA-A2–SLYNTVATL diffraction data, the asymmetric dimer of heavy chains and β2m domains from a high resolution crystal structure of HLA-A2–influenza matrix epitope (unpublished data) was used as the search probe (with peptide coordinates omitted) and yielded unambiguous solutions of R_{cryst} of ~45% (R_{free} ~46%) for data between 30 and 4Å. A Fo-Fc difference map revealed clearly the presence of the antigenic peptides. The difference in peptide conformation between HLA-A2–SLFNTVATL and HLA-A2–SLYNTVATL was unambiguous.

Using the CNS program (33) HLA-A2–SLFNTVATL and HLA-A2–SLYNTVATL were subjected to several rounds of rigid body refinement of individual domains (α1, α2, α3, β2m), and the peptides were modeled into Fo-Fc difference density maps using program O (34). Further rounds of refinement were performed using standard CNS protocols for bulk solvent correction and overall anisotropic B-factor scaling, positional refinement, simulated annealing, and individual B-factor refinement. Manual refitting of the models was performed using O, and water molecules were added based on peaks that were at least 3.0 σ in height in Fo-Fc density maps. Program REFMAC (35) was used for a final round of refinement with program ARP/wARP to add an additional set of bound water molecules (36). Structural superpositions were performed using program SHP (37). Fig. 4 was prepared using program BobScript (38).

T2 Peptide Binding Assay. A TAP-deficient T2 cell line was used to assess the ability of HLA-A2 to bind each of the variant peptides (39, 40). In brief, 10^5 T2 cells were incubated with 300 μM of each of the peptide variants overnight for 16 h at 37°C in serum-free RPMI 1640 medium in flat-bottom 96-well plates. Cells were transferred to round-bottom 96-well plates the next day and washed with PBS. Cells were stained for HLA-A2 by immunofluorescence using FITC-labeled mAB BB7.2 (anti–HLA-A2; BD Biosciences). Results were determined by FACS sorting.

Surface Plasmon Resonance. Surface plasmon resonance studies were performed using a BIAcore 2000 (Biacore AB) as described previously (41). HLA-A2–SLFNTVATL and HLA-A2–SLYNTVATL were enzymatically biotinylated on COOH-terminal BirA recognition and immobilized to CM5 sensor chips via covalently coupled streptavidin (41). Kinetic constants were derived using the curve-fitting facility of the BIAevaluation program (Version 3.0; BIAcore) and rate equations were derived from the simple 1:1 Langmuir binding model (A + B→AB). Other curve fitting was performed in Origin version 5 (MicroCal). Equilibrium thermodynamic constants were obtained by measuring the ΔG^o over a range of temperatures and fitting to these data the nonlinear form of the van't Hoff equation (42),

$$\Delta G^\circ = \Delta H_{To} - T \times \Delta S_{To} + \Delta C_p(T - To) - T \times \Delta C_p \times \ln\left(\frac{T}{T_o}\right),$$

where T is the temperature in Kelvin (K); To is an arbitrary reference temperature (e.g., 298.15 K); ΔG° is the standard free energy of binding at T (kcal.mol^{-1}) and is calculated from the equilibrium dissociation constant (Kd); ΔH_{To} is the enthalpy change upon binding at To (kcal.mol^{-1}); ΔS_{To} is the standard state entropy change upon binding at To (kcal.mol^{-1}.K^{-1}); and ΔC_p is the change in heat capacity (kcal.mol^{-1}.K^{-1}) and is assumed to be temperature independent.

Thermodynamic constants for the transition state were determined by measuring the rate constants over a range of temperatures (43). According to transition state theory,

$$\ln\left(\frac{k_{rate}}{T}\right) = \ln\left(\frac{k_B}{h}\right) + \frac{\Delta^\ddagger S}{R} - \frac{\Delta^\ddagger H}{RT},$$

where k_{rate} is a first order rate constant (e.g., either k_{off} or k_{on} C° where C° is the standard state concentration [1 M]); k_B is the Boltzmann constant (3.3×10^{-24} cal.K^{-1}); h is the Plank constant (1.6×10^{-34} cal.s); R is the gas constant (2 cal.K^{-1}mol^{-1}); and $\Delta^\ddagger H$ and $\Delta^\ddagger S$ are the enthalpy and standard state entropy of activation, respectively. $\Delta^\ddagger H$ and $\Delta^\ddagger S$ are determined from the slope and intercept, respectively, of a plot of $\ln(k_{rate}/T)$ against 1/T.

Online Supplemental Material. Figs. S1 and S2 show peptide titration assays which were performed for the index peptide and peptide variants in the ELISPOT assay over a range from 10 to 0.008 μM, and in the chromium release assay over a range of 10^{-5}–10^{-11} M, respectively, to determine the optimal peptide concentration. The overall recognition patterns to all 171 peptide variants measured in the cytotoxicity assay for the two clones are summarized in Fig. S3. Functional correlation between the responses to the peptide variants in the ELISPOT and cytotoxicity studies is shown in Fig. S4. Online supplemental material is available at http://www.jem.org/cgi/content/full/jem.20041251/DC1.

Results

Fine Specificity of SLFNTVATL Recognition by CD8$^+$ T Cells. We selected two T cell clones, specific for the SLFNTVATL peptide presented by HLA-A2, that expressed completely different T cell receptors: clone G10 carried a Vα 28.1 (CDR3 α-loop region sequence CAVLGNSGNTPLV) and Vβ 5.1 (CDR3 β-loop region se-

Table I. *Crystallographic Statistics*

	SLFNTVATL	SLYNTVATL
Data collection		
Space group	P1	P1
Unit cell		
Dimensions (Å) (a, b, c)	47.9, 60.7, 71.1	48.1, 60.1, 71.2
Angles (°) (α, β, γ)	81.8, 76.2, 77.7	82.0, 76.2, 78.1
Source	SRS BM14-2	SRS BM14-2
Resolution (Å) (highest resolution shell)	20 − 1.6 (1.66 − 1.60)[a]	20 − 1.6 (1.66 − 1.60)[a]
Measured reflections	528,451	518,711
Unique reflections	99,884	101,373
Completeness (%)	93.5 (64.6)[a]	92.4 (58.8)[a]
I/σ (I)	14.0 (1.7)[a]	21.2 (2.1)[a]
R_{merge} (%)[b]	6.0 (45)[a]	3.5 (31)[a]
Refinement statistics		
Resolution range (Å)	20 − 1.6 (1.66 − 1.60)[a]	20 − 1.6 (1.66 − 1.60)[a]
R_{cryst}[c]	21.0	21.5
R_{free}[d]	24.1	24.1
No. of residues	768	768
No. of water molecules	755	768
Rms deviation from ideality		
Bond lengths (Å)	0.015	0.016
Bond angles (°)	1.54	1.62
Ramachandran plot (%) (favored, allowed, generous, disallowed)	(91.3, 8.4, 0.3, 0.0)	(93.5, 7.2, 0.3, 0.0)

[a]Numbers in parentheses correspond to the outermost shell of data.
[b]$R_{merge} = \Sigma_{hkl} | I - \langle I \rangle | / \Sigma_{hkl} | I |$ where I is the intensity of unique reflection hkl and $\langle I \rangle$ is the average over symmetry-related observations of unique reflection hkl.
[c]$R_{cryst} = \Sigma | F_{obs} - F_{calc} | / \Sigma | F_{obs} |$ where F_{obs} and F_{calc} are the observed and calculated structure factors, respectively.
[d]R_{free} is calculated as for R_{cryst} but using 5.0% of reflections sequestered before refinement.

quence CASSFDAEAF) TCR, and clone T5-004 used Vα 2.1 (CDR3 α-loop region sequence CAFPSGYALN) and Vβ 2.3 (CDR3 β-loop region sequence CATSSTGTGGGETQY). These clones were tested in the ELISPOT assay with 171 variant peptides of the SLFNTVATL epitope, each differing by one amino acid from the index peptide sequence. Thus, all possible single amino acid changes to the SLFNTVATL epitope were tested for recognition. The results (Fig. 1) indicate that less than one third of these single amino acid variant peptides were recognized, with similar patterns of response for the two clones. Virtually identical results were obtained in a CTL lysis assay (Figs. S1 and S2, available at http://www.jem.org/cgi/content/full/jem.20041251/DC1). For both assays, the peptides were titrated and the concentrations used were chosen to be the lowest that gave maximal recognition of the parent peptide (Figs. S3 and S4, available at http://www.jem.org/cgi/content/full/jem.20041251/DC1). It is noteworthy that, like the total response in approximately half of HLA-A2$^+$ HIV-infected people, these T cell clones cross-reacted between the A subtype SLFNTVATL and B subtype SLYNTVATL sequences.

To determine to what extent failure of the peptide to bind HLA-A2 contributed to nonrecognition by the T cells, we titred each peptide for its ability to stabilize surface expression of HLA-A2 on the T2 cell line (39, 40). The SLFNTVATL and SLYNTVATL peptides reached maximum HLA-A2 stabilization at 200–300 μM. Other peptides tended to bind less well but the level of HLA-A2 expression observed at peptide concentration of 300 μM gave a qualitative assessment of whether a peptide bound (Fig. 2). Most (74.5%) peptides bound to a measurable extent and 29 out of the 51 that gave undetectable binding were altered at the main anchor positions, 2 and 9 for peptides presented by HLA-A2. 65.5% of the peptides that were seen by neither clone gave detectable binding (>5% increased expression compared with the index peptide), suggesting that nonrecognition could be attributed to inade-

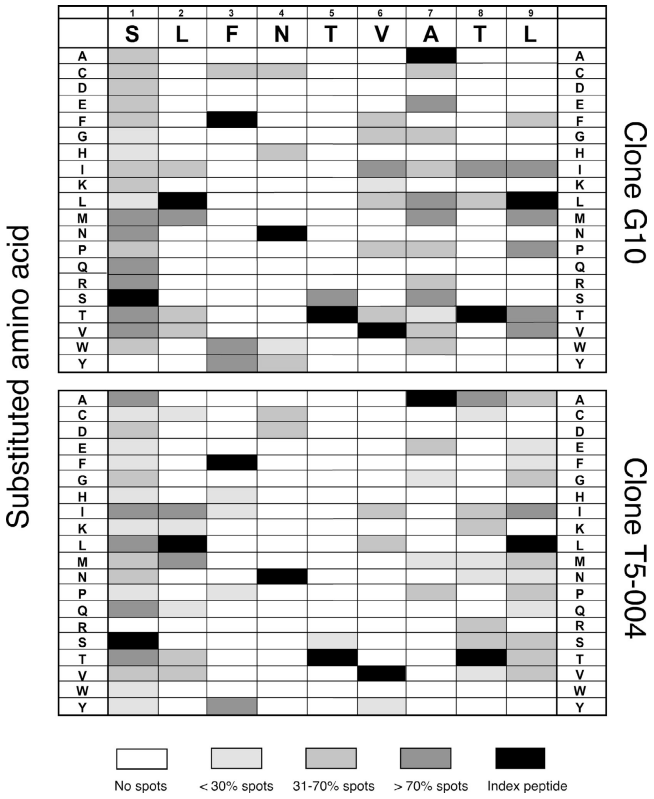

Figure 1. Recognition pattern of monosubstituted SLFNTVATL peptide variants by two different CTL clones. Clones G10 and T5-004 from two different HIV$^+$ donors were tested for their capacity to recognize peptide-pulsed HLA-A2 B cells by measuring IFN-γ secretion in the ELISPOT assay. Every one of the 20 genetically coded amino acids was substituted in each of the nine possible positions in the HLA-A2–restricted epitope SLFNTVATL (total of 171 peptide variants). The residues of the index peptide SLFNTVATL are listed horizontally at the top of the chart; the letters along the sides indicate the residues replacing the index residue. Results were expressed as a ratio of the percentage of SFU as compared with the index peptide (SLFNTVATL). Responses were graded as corresponding shades in the boxes. This assay was repeated three to five times for each variant peptide, with each experiment yielding the same pattern of peptide recognition. Background counts for negative control wells without peptides were always <5 SFU/well.

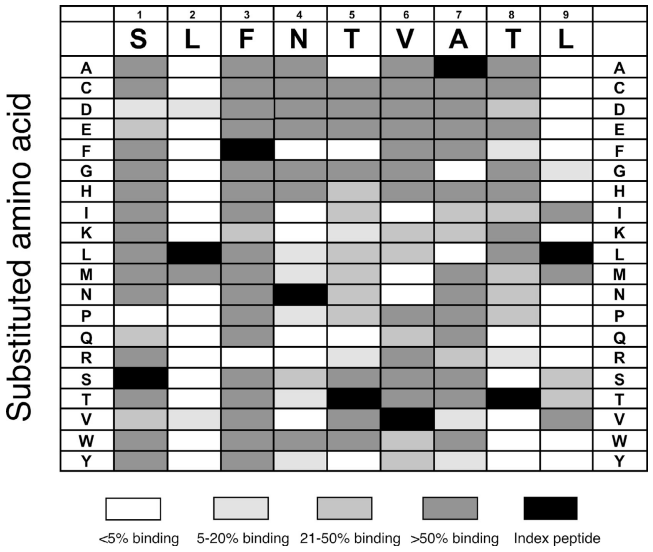

Figure 2. Binding of peptide variants to HLA-A2. All 171 single amino acid substitution peptide analogues of SLFNTVATL were tested for binding to HLA-A2 using TAP-deficient T2 cells. Results were determined by flow cytometry analysis. Peptide variants were compared with the index peptide SLFNTVATL, and results were expressed as a percentage of the mean fluorescence. Relative binding strengths were graded into the corresponding shades in the boxes.

quate contact of bound peptide with the T cell receptor. 17 peptides (S1P, L2C, L2I, L2K, L2Q, L2T, V6I, A7G, A7L, T8S, T8V, L9A, L9E, L9F, L9N, L9P, L9Q) out of the 51 that gave undetectable binding were seen by at least one T cell clone, consistent with T cells' ability to respond to very low numbers of epitope peptide on MHC molecules (44, 45). Thus, much of the nonrecognition by T cells of peptides altered at residues 3–8 represents failure of the T cell receptor to engage with a bound peptide.

Although the clones from two different donors were thought to be representative, we also tested uncloned PBMCs from two further HIV$^+$ donors (Fig. 3). These responses were similarly highly sensitive to variation in the epitope, but showed cross-reactivity to the A subtype SLFNTVATL and B subtype SLYNTVATL epitopes (Fig. 3, A and B). The clonality of this response was assessed by sorting SLFNTVATL- and SLYNTVATL-specific T cells from one of these donors using the respective tetramers and sequencing the TCRB CDR3 regions using unbiased anchored RT-PCR (28). We found that the SLFNTVATL-specific T cells comprised two clones, defined by different TCR BV sequences, one more frequent than the other (Fig. 3 C). The SLYNTVATL-specific T cells comprised one clone, which was identical in its expressed TCRB locus, to the dominant SLFNTVATL-specific clone (Fig. 3 C). Thus, the two clones dominating this response showed very fine specificity when confronted with each of the peptide variants, similar to results with the cloned T cells.

Structure of HLA-A2 with SLFNTVATL and SLYNTVATL. We embarked on structural analysis of HLA-A2–SLFNTVATL and HLA-A2–SLYNTVATL to provide structural contexts for interpretation of the functional effects of single amino acid changes to the peptides (26). We succeeded in crystallizing HLA-A2 bound to both peptides and determined the two crystal structures at high resolution (1.6 Å).

The structure of SLFNTVATL bound to HLA-A2 is shown in Fig. 4 A. As in previous nonamer peptide–HLA-A2 structures (46), peptide positions 2 and 9 are major anchors, with L2 deeply buried in the B pocket and L9 in the F pocket, whereas position 3 is a secondary anchor, with F3 inserted into the D pocket. As reported before, many variant peptides with single amino acid changes at residues 3–8 retained the ability to bind HLA-A2, but were not recognized by T cells. In this region of the bound SLFNTVATL peptide, the side chains of residues 4, 6, and 8 are highly exposed to solvent (and TCR recognition), the side chains of residues 3 and 7 are partially exposed, and the side chain of residue 5 is orientated down-

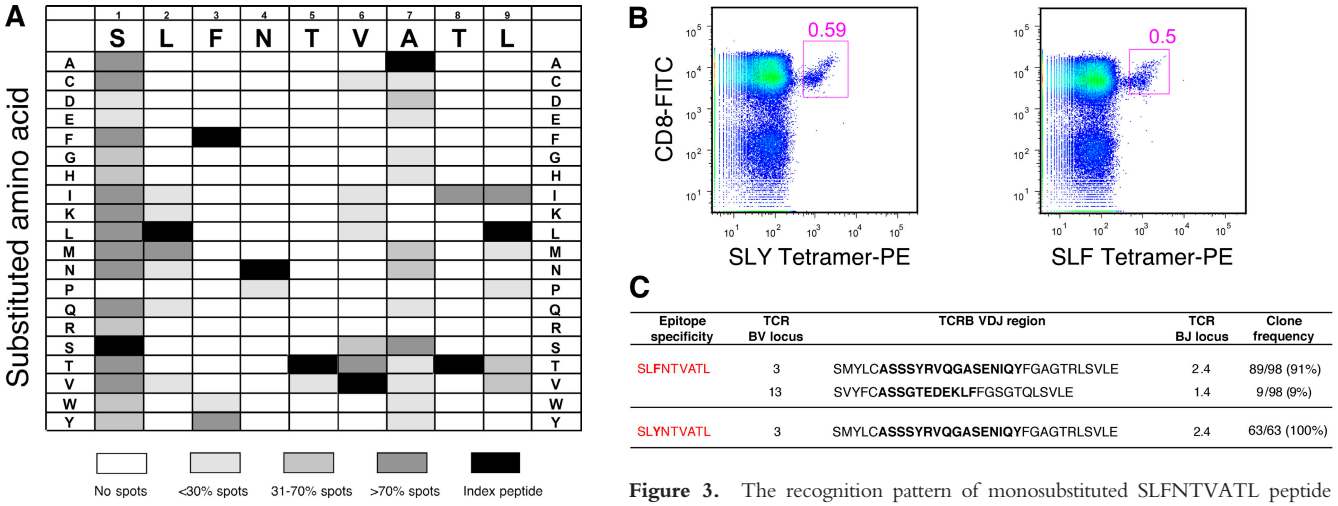

C

Epitope specificity	TCR BV locus	TCRB VDJ region	TCR BJ locus	Clone frequency
SLFNTVATL	3	SMYLC**ASSSYRVQGASENIQY**FGAGTRLSVLE	2.4	89/98 (91%)
	13	SVYFC**ASSGTEDEKLF**FGSGTQLSVLE	1.4	9/98 (9%)
SLYNTVATL	3	SMYLC**ASSSYRVQGASENIQY**FGAGTRLSVLE	2.4	63/63 (100%)

Figure 3. The recognition pattern of monosubstituted SLFNTVATL peptide variants by PBMCs from an HIV$^+$ patient and clonotype analysis. (A) PBMCs from an HIV$^+$ patient (who was not the donor of either T cell clone) were tested for recognition of SLFNTVATL and single amino acid variants in the ELISPOT assay. Results were expressed as percentage of SFU as compared with the index peptide. Responses were graded as corresponding shades in the boxes. Background counts for negative control wells without peptides were always <5 SFU/well. (B) Tetramer staining of SLFNTVATL or SLYNTVATL-specific CD8$^+$ T cells from PBMCs of the HIV$^+$ patient. Tetramer$^+$ cells were flow cytometrically sorted and subjected to TCRB sequence analysis. (C) TCRB sequences of SLFNTVATL and SLYNTVATL-specific CD8$^+$ T cells from B and their frequency in the total number of bacterial colonies sequenced.

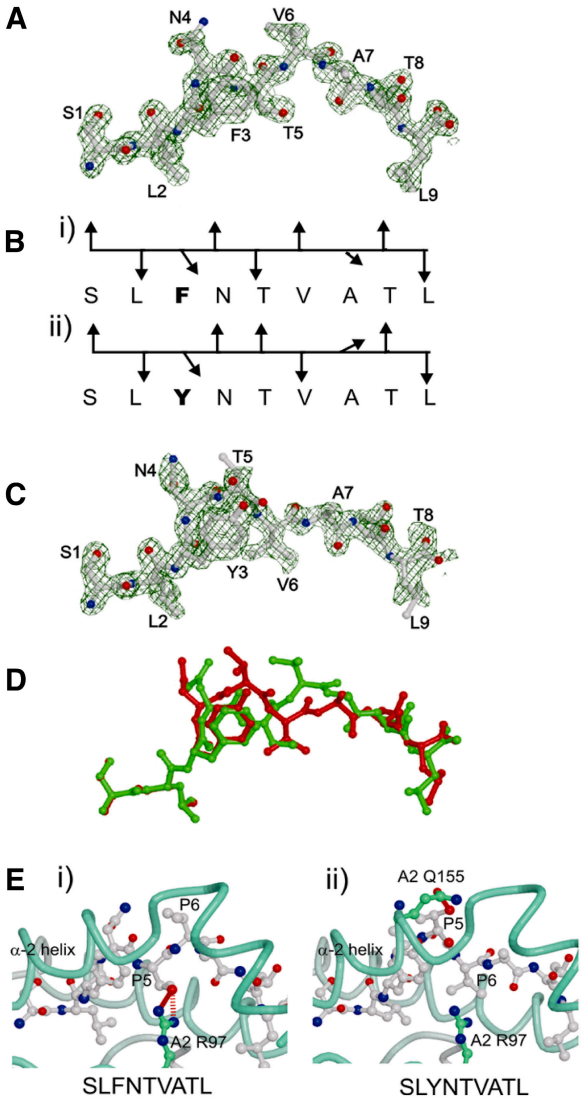

ward into the peptide binding groove (Fig. 4, A and B). The main chain conformation for the central region of peptides bound to HLA-A2 is highly variable (46), but the available crystal structures for nonamer peptides bound to HLA-A2 indicate that it is common for one of the side chains of residues 5, 6, or 7 to point down into the binding groove (46–48). Conversely, an absence of stabilizing contacts between MHC and peptide in this region has been associated with poor peptide binding affinity (49). The conformation of SLFNTVATL bound to HLA-A2 is similar to that of the HIV-1 gp120 epitope TLTSCNTSV reported by Madden et al. (46, PDB accession code 1HHG; reference 46).

Similar to a previous, systematic study of the effect of single amino acid substitutions on T cell recognition of a peptide–HLA-A2 complex, the nonrecognition of peptides altered at P3-P8 can result from direct or indirect changes at the TCR recognition surface (11). On the basis of the bound structure of the index peptide SLFNTVATL, substitutions at the highly exposed side chains of residues 4, 6, and 8 may result in direct changes to interactions with TCRs. However, T cell recognition appears to be equally, if not more, sensitive to substitutions to the buried side

Figure 4. Structural differences between SLFNTVATL and SLYNTVATL peptide conformations in HLA-A2. (A) 2Fo-Fc electron density for SLFNTVATL and (C) SLYNTVATL peptides are shown as green chicken wire (contoured at 1.2 σ) viewed in profile through the HLA-A2 α2 helix. (B) General side chain orientation for the two peptides as viewed in profile through the α2 helix. (D) Comparison of SLFNTVATL (green) and SLYNTVATL (red) peptide structures by superimposition of the two binding grooves, illustrating the diametric apposition of the P5 and P6 side chains of the two peptides. (E) Diagram illustrating the two different hydrogen-bonding arrangements of the P5 threonine with the HLA-A2 molecule: (i) The interaction of SLFNTVATL P5 threonine with R97, and (ii) the interaction of SLYNTVATL P5 threonine with Q155. These interactions appear to lock the peptides into their discrete conformations. Hydrogen bonds are denoted as red dashes.

chain of residue 5. In the index peptide, the side chain of T5 makes a hydrogen bond with arginine at position 97 in the floor of HLA-A2 groove (Fig. 4 E); the only variant at this position recognized by the T cells was serine (Fig. 1), which would be able to make an identical hydrogen bond. Other P5 variants bound HLA-A2 (Fig. 2), but were not recognized by the T cells. This would be consistent with a change in hydrogen bonding of the P5 side chain, causing changes in the bound conformation of the peptide such that TCRs specific for the native sequence cannot interact. On the basis of the first set of peptide–HLA-A2 crystal structures, Madden et al. (46) suggested that single amino acid substitutions could alter the entire conformation of the bound peptide. Subsequent studies have demonstrated that even subtle changes in anchor residues can change the pMHC surface (i.e., as in the HLA-B8 HIV-1 gag p17 [24–31] structure, substitution of arginine for lysine at the position five anchor [50]).

The structure determination of HLA-A2–SLYNTVATL unexpectedly confirmed that single amino acid substitutions at secondary anchor positions could exert profound effects on the overall conformation of the SLFNTVATL peptide. Comparison of the structures of HLA-A2–SLFNTVATL and HLA-A2–SLYNTVATL revealed a substantial difference in the conformations of the peptides (Fig. 4). As a result of a switch in main chain conformation for the central portion of the SLYNTVATL peptide, the positions of the T5 and V6 side chains were flipped by ~180 degrees. The P5 threonine–HLA-A2 R97 hydrogen bond is exchanged for a hydrogen bond between P5 threonine and HLA-A2 Q155 (Fig. 4 E). This change in conformation is not forced by any potential steric clash resulting from the addition of the side chain hydroxyl group on substitution of phenylalanine with tyrosine. Instead it appears to be the result of the changed electrostatic environment of the binding groove no longer favoring polar interactions with the P5 threonine over hydrophobic interactions with the P6 valine. The balance of polar and hydrophobic interactions determining the choice of this conformation for SLYNTVATL, in preference to the conformation adopted by SLFNTVATL, is subtle, but there is no evidence of mixed conformations for either peptide in the respective crystal structures. The 1.6-Å resolution of both crystallographic datasets leaves no doubt that the two peptide structures are distinct and correct. Both structures were derived from crystals grown under identical conditions and were of the same space group (P1) and unit cell dimensions. The crystallographic asymmetric unit contained two copies of the HLA-A2–peptide molecules with the peptides adopting a common conformation, and there were no direct lattice contacts involving the peptides. The HLA-A2–SLFNTVATL structure was determined three times: twice in the P1 space group crystal form to give structure, at pH 6.5 and pH 7.4 (both to 1.6 Å resolution), and once in a $P2_1$ space group crystal form, at pH 7.4 (1.5-Å resolution with two molecules in the asymmetric unit; unpublished data). In each case, the SLFNTVATL peptide clearly adopted exactly the same conformation.

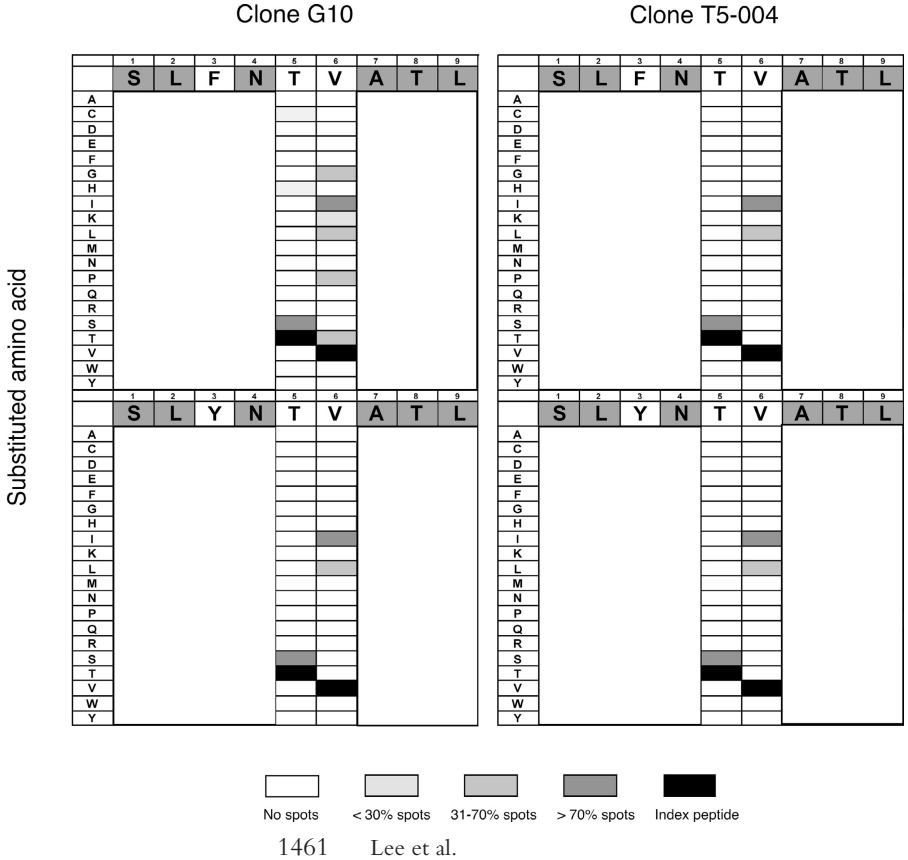

Figure 5. Comparison of clonal responses to P5 and P6 variants of SLFNTVATL and SLYNTVATL. Clones G10 and T5-004 were tested for the recognition of single amino acid substitution peptide analogues of SLYNTVATL, in which the residues at P5 and P6 were substituted by all of the 19 other amino acids. The P5 and P6 peptide variants were tested for the capacity to sensitize HLA-matched B cells to induce IFN-γ production in the ELISPOT assay as described before. Responses were compared relative to the index peptide SLYNTVATL and graded into four groups as shown. The overall recognition patterns to the P5 and P6 peptide variants of SLYNTVATL and corresponding SLFNTVATL-derived variants are nearly identical for the two clones.

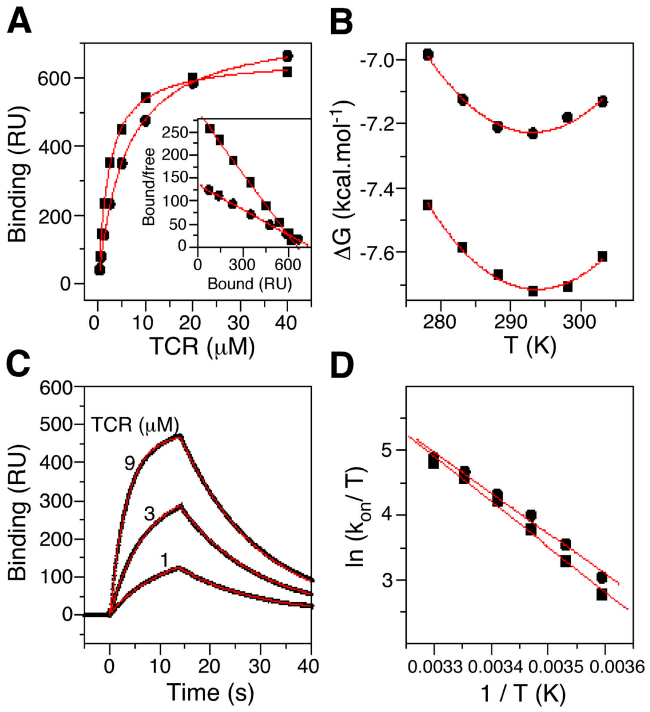

Figure 6. Binding of clone G10 TCR to HLA-A2–SLFNTVATL and HLA-A2–SLYNTVATL. (A) Measurement of affinity. Soluble G10 TCR was injected at the indicated concentrations over surfaces onto which ~1,000 RU of HLA-A2–SLFNTVATL or HLA-A2–SLYNTVATL were immobilized and the level of binding reached at equilibrium was recorded. The lines are fits of the simple 1:1 binding model that yielded affinities of Kd 5.2 μM and 2.2 μM for HLA-A2–SLFNTVATL (circles) and HLA-A2–SLYNTVATL (squares), respectively. (inset) Scatchard transformation of the same data. (B) van't Hoff analysis. Affinities (converted to ΔG° as in Table II) were measured over a range of temperatures. The curves show fits of the nonlinear van't Hoff equation to the data. These fits were used to determine the ΔH, $-T\Delta S$, and ΔC values shown in Table II. (C) Kinetic analysis. The indicated concentrations of G10 TCR were injected over HLA-A2–SLYNTVATL (black lines). A simultaneous global fit of equations derived from the simple 1:1 binding model is shown (red). This yielded a k_{on} of 24900 $M^{-1}.s^{-1}$ and a k_{off} of 0.064 s^{-1}. (D) Eyring plot of k_{on} measured at different temperatures. The slope and intercept of linear fits to the data (red lines) were used to determine $\Delta^{\ddagger}H_{on}$ and $T\Delta^{\ddagger}S_{on}$, respectively (Table II).

T Cell Recognition of Variants at Positions 5 and 6 in SLFNTVATL and SLYNTVATL. The T cell clones we used, and approximately half the polyclonal T cell responses in HIV-infected people with HLA-A2, cross-react with SLFNTVATL and SLYNTVATL. Given the very fine specificity requirements for these responses in the recognition experiments, T cell cross-reactivity for this variant seemed to be at odds with the crystallographic findings. Therefore, we made and tested, using the two T cell clones, each of the 38 variants at positions 5 and 6 for both index peptides. The results show that the patterns of recognition were identical for clone T5-004 and very similar for clone G10 (Fig. 5). This implies that the side chains P5 and P6 are in the same position for T cell receptor interaction for both the P3F and P3Y epitopes. This could be explained by conformational changes in one or both peptides upon TCR binding, with the peptides adopting the same conformation in the TCR–peptide–MHC complex.

Kinetic Studies of TCR Binding to HLA-A2 Complexed with SLFNTVATL or SLYNTVATL. Conformational adjustments are known to occur at the binding interface when TCR engages pMHC (11, 30, 51–56). Conformational changes at binding interfaces can either precede or follow binding, as recently reviewed by Goh et al. (57). When they precede binding, there is a preexisting equilibrium between different conformational isoforms, one of which is compatible with binding. Because this is usually a minor isoform, the association rate constant (k_{on}) is typically slow. In contrast, when conformational changes follow binding, which is referred to as induced fit, the k_{on} is less likely to be slow. The slow k_{on} measured for TCR–pMHC interactions is evidence that, at least in some cases, these conformational changes precede TCR binding (41, 58, 59). It is also possible that conformational changes follow initial TCR engagement, as has been proposed by Wu et al. (60), but direct evidence for this is lacking. To investigate when the conformational change that we had identified occurred, we undertook a detailed kinetic and thermodynamic analysis of a TCR binding to these peptide variants. We expressed and purified a soluble form of the G10 TCR and tested this for binding to HLA-A2 presenting either SLFNTVATL or SLYNTVATL. Binding was measured at temperatures from 5 to 37°C. From the data, we determined thermodynamic and kinetic parameters for these interactions (Fig. 6 and Table II). If conformational changes preceded binding, we would have expected there to be differences in the association kinetics given that one of the peptides would have to undergo a substantial change before binding. However, in both cases, association fol-

Table II. *Summary of Binding Data*

Parameter[a]	SLFNTVATL	SLYNTVATL
Kd (μM)[b]	5.2 ± 0.5	2.2 ± 0.5
k_{on} ($M^{-1}.s^{-1}$)	34,000 ± 3,000	33,000 ± 5,000
k_{off} (s^{-1})	0.16 ± 0.002	0.06 ± 0.001
ΔG°[c]	−7.2	−7.7
ΔH[d]	−10.4 ± 0.4	−10.5 ± 0.4
$-T\Delta S$[d]	3.2 ± 0.5	2.8 ± 0.4
ΔC (kcal.$M^{-1}.K^{-1}$)	0.62 ± 0.05	0.63 ± 0.05
$\Delta^{\ddagger}H_{on}$[e]	12.5 ± 0.6	13.7 ± 0.7
$-T\Delta^{\ddagger}S_{on}$[e]	−1.1 ± 0.7	−2.4 ± 0.7

[a]All parameters were measured/calculated at 25°C (298.15 K) and expressed in kcal.M^{-1} unless otherwise indicated. Unless otherwise indicated, values shown are mean ± SEM ($n \geq 3$).
[b]Measured by equilibrium binding analysis (Fig. 6 A).
[c]ΔG° = R.T.lnKd, where R is the gas constant and Kd is the equilibrium dissociation constant expressed in units M.
[d]Determined by van't Hoff analysis (Fig. 6 B). Values are mean ± SE of fit.
[e]Determined by Eyring analysis (Fig. 6 D). Values are mean ± SE of fit.

lowed pseudo–first order kinetics and the k_{on}s were indistinguishable. Nor were any differences detected in the activation enthalpy ($\Delta^{\ddagger}H_{on}$) and entropy changes ($T\Delta^{\ddagger}S_{on}$) that accompany association. The G10 TCR dissociated more slowly from the HLA-A2–SLYNTVATL complex, resulting in an approximately twofold higher affinity. To confirm that the k_{on}s were similar for HLA-A2–SLFNTVATL and HLA-A2–SLYNTVATL under conditions nearest to the crystallization conditions, we measured binding at 50 mM MES, pH 6.5, with no NaCl present. Association rate constants under these conditions were essentially identical, despite the large differences observed in the two peptide-HLA-A2 crystal structures at these conditions. Therefore, our analysis of the association kinetics suggests that no energetically significant conformational changes in the peptide occur before formation of the transition state complex. This implies that conformational changes follow formation of the transition state, supporting an induced fit mechanism of conformational change.

Discussion

Our results make two important and related points. First, the data show the exquisite functional specificity of $CD8^+$ T cells, with different receptors from chronically HIV-infected patients, to variants of this immunodominant epitope. Second, we provide evidence in support of an induced fit mechanism of TCR binding, whereby large conformational changes in the peptide follow initial TCR engagement.

Whether $CD8^+$ T cells cross-react with virus variants is a very important issue in infection with HIV and other variable viruses. Failure of T cells to recognize variants gives the chronically replicating virus multiple chances to escape from immune control. Here, we show that for a clinically relevant epitope, two thirds of random mutations are not recognized. Although much has been made of cross-reactive T cells in the arena of vaccine design, our data are in line with earlier studies on peptide variants of influenza matrix peptide presented by HLA-A2, HTLV-1 tax peptide presented by HLA-A2 and EBV EBNA-3 peptide presented by HLA-B8 (9–11). Therefore, T cell responses to pathogenic viruses appear very sensitive to epitope change. However, Mason (61) has argued that because the T cell receptor repertoire is limited by the total number of T cells in the body, yet responds to all pathogens, each receptor must be able to see many different peptides presented by the same MHC molecule. Indeed, there are well-known examples of T cell clones cross-reacting on different MHC–peptide complexes (3, 4), but the specific set of binding interactions made by the TCR to each of these peptide–MHCs must be different (56, 62) and we would expect each binding mode to be just as sensitive to variants of the relevant peptide. Thus, the paradox of the same TCR showing significant cross-reactivity, but also very fine specificity for recognition of a single epitope, can be resolved. For a minority of variant peptides, binding to the MHC is so impaired that the epitope fails to present. Most well-described escape mutations of HIV are of this type (13–18, 50) and such mutations reach fixation. However, we show here that most variant peptides still bind HLA-A2, but most are not recognized by T cells. Given that T cells can react to very low numbers of presented peptides on a cell (44, 45), this finding implies that the majority of randomly generated epitope mutations affect the interaction between TCR and bound peptide. Priming of new T cell clones could deal with the problem, but in ongoing HIV infection the capacity to make new primary T cell responses may be impaired (22), possibly because of damage to dendritic cells or T helper cells. If we can generalize from our findings concerning a dominant HIV epitope, and from previous studies of this type, the implication is that a T cell response to HIV that fails to suppress virus replication sufficiently is doomed to select escape mutants. The demonstration that the HLA type of an infected person shapes the virus sequence is powerful support for this concept (63).

One surprising finding in our structure–function analysis was that the apparently small variation in the epitope from SLFNTVATL to SLYNTVATL (a common mutation in vivo that is cross-recognized by many T cells) causes a major difference in structure. Yet the observed T cell cross-reactivity implies that one conformation, common to SLFNTVATL and SLYNTVATL, is recognized by the TCRs. This interpretation is strongly supported by the very similar patterns of T cell recognition for variants of the two peptides in which single amino acid changes are made to residues in the conformationally different regions. If peptides with either conformation pre–TCR-binding change to a single common conformation on TCR binding, the additional changes in peptide sequence would be sampled in essentially identical contexts. The alternative explanation, that both TCRs recognize two very different peptide structures and that many changes in the structurally distinct portions (P5-P6) of these peptides coincidently all have the identical effect on TCR recognition, is highly implausible. It follows that at least one of the peptides must undergo a substantial conformational change during TCR binding. Some previous observations support this hypothesis. Crystal structures of HLA-A2 HTLV-1 Tax epitope in complex with two different TCRs show a significant and identical change in the peptide conformation on comparison of the pMHC and TCR–pMHC structures (52, 64). In that case, the change in peptide conformation at P5-P6 rotated both side chains by $\sim 90^{\circ}$ on TCR binding. A subsequent series of crystal structures for TCR–pMHC complexes of altered peptide ligands also preserved the same TCR bound peptide conformation (65). Clearly, the balance of interactions that determine the conformation of the central portion of the peptide in at least some pMHCs can be altered in response to TCR binding. For SLFNTVATL and SLYNTVATL kinetic analysis revealed, somewhat unexpectedly, that the k_{on}s (and the $\Delta^{\ddagger}H_{on}$) of TCR binding the two peptide complexes were indistinguishable. Because significant conformation adjustment of the peptide would result in significant differences in the k_{on} and/or $\Delta^{\ddagger}H_{on}$, this implies that energetically significant conformational adjustments are not occurring before formation of the transition state

complex. This means that the conformational changes probably occur as the transition state complex relaxes into the final complex. An unlikely alternative explanation for the identical kinetics is that both peptides change into a third common conformation in the transition state, and that, by coincidence, both conformational changes have identical energetic barriers.

All interacting molecules, including the TCR–pMHC complex form a high-energy transition state complex (66) before relaxing into the final complex, and Wu et al. (60) showed that the TCR forms contact with residues on the MHC α-helices in the transition state complex. They were unable to rule out formation of contacts with peptides in the transition state, but it was clear that TCR forms these in the final complex. Based on these findings, and structural studies of other TCR–pMHC systems, which provide clear evidence of conformational change upon binding, Wu et al. proposed that the TCR initially forms contacts with the MHC in the transition state, and that after this there is a conformational change of the TCR CDR3 loops and formation of contacts with peptide (60). However, they provided no direct evidence for this induced fit mechanism and their data are also consistent with a preexisting equilibrium mechanism (57), whereby conformational changes precede TCR binding to pMHC. Indeed, the very slow k_{on} of many TCR–pMHC interactions (59), including the 2B4 TCR system studied by Wu et al., strongly suggests that conformation changes often precede formation of the transition state. Recently, Gakamsky et al. (67) pointed out that published kinetic and structural data to date do not allow one to distinguish between the two main mechanisms of conformational change at the TCR–pMHC interface.

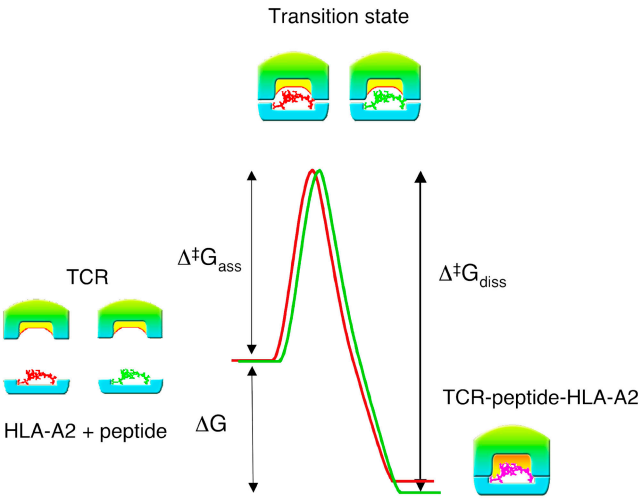

Figure 7. Thermodynamic analysis of TCR binding to HLA-A2–SLFNTVATL and HLA-A2–SLYNTVATL. Reaction profile illustrating the energy changes as the G10 T cell receptor binds to HLA-A2 complexed to SLFNTVATL and SLYNTVATL. ΔG^{ass} measures the total height of the transition state barrier. $\Delta G = \Delta H$ (enthalpic) $+T\Delta S$ (entropic) (Fig. 6). The figure illustrates the conformational changes in the peptides occurring as the transition state loose complex relaxes into the final bound TCR–peptide–MHC complex.

In contrast, the data presented here provide evidence that conformational changes at the TCR–pMHC binding interface can occur after formation of the transition state complex (Fig. 7). These findings support the proposal by Wu et al. that the TCR first docks on MHC molecules relatively independently of the peptide, followed by conformational adjustments as the TCR and peptide–MHC relax from the transition state into the final complex. The stability of the final complex and, therefore, TCR triggering will be very sensitive to epitope sequence variation.

In conclusion, these studies give some insight into how initial TCR contact can be quite cross-reactive, but transient. If TCR and peptide–MHC can adjust conformation to fit each other, more stable binding occurs and the T cell is triggered. However, this phase of T cell activation is highly specific with minimal scope for cross-reactivity. Such fine specificity may protect the host from autoimmune reactions but a penalty is paid when a virus can persist and is poorly controlled, as replication and mutation will lead to frequent immune escape. For vaccine design, the susceptibility of T cells to virus variation is of immense importance (24, 25). Unless vaccines can stimulate very broad T cell responses specific for multiple epitopes, it is unlikely that vaccines that are based on one subtype will offer significant protection against another subtype of HIV where the proteins differ by 20–30% (i.e., more than one amino acid change per epitope). Even within subtypes, there is enough variation (~5%) to cause concern.

The authors thank the staff at the Synchrotron Radiation Source for assistance with X-ray data collection.

This work was funded by the National Institutes of Health–University of Oxford Scholars Program, the Medical Research Council, and in part by the International AIDS Vaccine Initiative. E.Y. Jones is a Cancer Research UK Principal Research Fellow.

The authors have no conflicting financial interests.

Submitted: 23 June 2004
Accepted: 25 October 2004

References

1. Huesmann, M., B. Scott, P. Kisielow, and H. von Boehmer. 1991. Kinetics and efficacy of positive selection in the thymus of normal and T cell receptor transgenic mice. *Cell.* 66: 533–540.
2. Ignatowicz, L., J. Kappler, and P. Marrack. 1996. The repertoire of T cells shaped by a single MHC/peptide ligand. *Cell.* 84:521–529.
3. Burrows, S.R., S.L. Silins, R. Khanna, J.M. Burrows, M. Rischmueller, J. McCluskey, and D.J. Moss. 1997. Cross-reactive memory T cells for Epstein-Barr virus augment the alloresponse to common human leukocyte antigens: degenerate recognition of major histocompatibility complex-bound peptide by T cells and its role in alloreactivity. *Eur. J. Immunol.* 27:1726–1736.
4. Lang, H.L., H. Jacobsen, S. Ikemizu, C. Andersson, K. Harlos, L. Madsen, P. Hjorth, L. Sondergaard, A. Svejgaard, K. Wucherpfennig, et al. 2002. A functional and structural basis for TCR cross-reactivity in multiple sclerosis. *Nat. Immunol.* 3:940–943.

5. Cecka, J.M., J.A. Stratton, A. Miller, and E. Sercarz. 1976. Structural aspects of immune recognition of lysozymes. III. T cell specificity restriction and its consequences for antibody specificity. *Eur. J. Immunol.* 6:639–646.
6. Carbone, F.R., B.S. Fox, R.H. Schwartz, and Y. Paterson. 1987. The use of hydrophobic, alpha-helix-defined peptides in delineating the T cell determinant for pigeon cytochrome c. *J. Immunol.* 138:1838–1844.
7. Hedrick, S.M., L.A. Matis, T.T. Hecht, L.E. Samelson, D.L. Longo, E. Heber-Katz, and R.H. Schwartz. 1982. The fine specificity of antigen and Ia determinant recognition by T cell hybridoma clones specific for pigeon cytochrome c. *Cell.* 30:141–152.
8. Dunham, E.K., S.F. Schlossman, and B. Benacerraf. 1974. Interactions between two antigens governed by the poly-L-lysine gene: failure of one to inhibit competitively an in vitro response to the other. *Proc. Soc. Exp. Biol. Med.* 145:537–541.
9. Gotch, F., A. McMichael, and J. Rothbard. 1988. Recognition of influenza A matrix protein by HLA-A2–restricted cytotoxic T lymphocytes. Use of analogues to orientate the matrix peptide in the HLA-A2 binding site. *J. Exp. Med.* 168: 2045–2057.
10. Burrows, S.R., S.L. Silins, D.J. Moss, R. Khanna, I.S. Misko, and V.P. Argaet. 1995. T cell receptor repertoire for a viral epitope in humans is diversified by tolerance to a background major histocompatibility complex antigen. *J. Exp. Med.* 182: 1703–1715.
11. Hausmann, S., W.E. Biddison, K.J. Smith, Y.H. Ding, D.N. Garboczi, U. Utz, D.C. Wiley, and K.W. Wucherpfennig. 1999. Peptide recognition by two HLA-A2/Tax11-19-specific T cell clones in relationship to their MHC/peptide/TCR crystal structures. *J. Immunol.* 162:5389–5397.
12. McMichael, A.J., and R.E. Phillips. 1997. Escape of human immunodeficiency virus from immune control. *Annu. Rev. Immunol.* 15:271–296.
13. Phillips, R.E., S. Rowland-Jones, D.F. Nixon, F.M. Gotch, J.P. Edwards, A.O. Ogunlesi, J.G. Elvin, J.A. Rothbard, C.R. Bangham, C.R. Rizza, et al. 1991. Human immunodeficiency virus genetic variation that can escape cytotoxic T cell recognition. *Nature.* 354:453–459.
14. Price, D.A., P.J. Goulder, P. Klenerman, A.K. Sewell, P.J. Easterbrook, M. Troop, C.R. Bangham, and R.E. Phillips. 1997. Positive selection of HIV-1 cytotoxic T lymphocyte escape variants during primary infection. *Proc. Natl. Acad. Sci. USA.* 94:1890–1895.
15. Goulder, P.J., R.E. Phillips, R.A. Colbert, S. McAdam, G. Ogg, M.A. Nowak, P. Giangrande, G. Luzzi, B. Morgan, A. Edwards, et al. 1997. Late escape from an immunodominant cytotoxic T-lymphocyte response associated with progression to AIDS. *Nat. Med.* 3:212–217.
16. Borrow, P., H. Lewicki, X. Wei, M.S. Horwitz, N. Peffer, H. Meyers, J.A. Nelson, J.E. Gairin, B.H. Hahn, M.B. Oldstone, and G.M. Shaw. 1997. Antiviral pressure exerted by HIV-1-specific cytotoxic T lymphocytes (CTLs) during primary infection demonstrated by rapid selection of CTL escape virus. *Nat. Med.* 3:205–211.
17. Evans, D.T., D.H. O'Connor, P. Jing, J.L. Dzuris, J. Sidney, J. da Silva, T.M. Allen, H. Horton, J.E. Venham, R.A. Rudersdorf, et al. 1999. Virus-specific cytotoxic T-lymphocyte responses select for amino-acid variation in simian immunodeficiency virus Env and Nef. *Nat. Med.* 5:1270–1276.
18. Barouch, D.H., J. Kunstman, M.J. Kuroda, J.E. Schmitz, S. Santra, F.W. Peyerl, G.R. Krivulka, K. Beaudry, M.A. Lifton, D.A. Gorgone, et al. 2002. Eventual AIDS vaccine failure in a rhesus monkey by viral escape from cytotoxic T lymphocytes. *Nature.* 415:335–339.
19. Betts, M.R., J. Krowka, C. Santamaria, K. Balsamo, F. Gao, G. Mulundu, C. Luo, N. N'Gandu, H. Sheppard, B.H. Hahn, S. Allen, and J.A. Frelinger. 1997. Cross-clade human immunodeficiency virus (HIV)-specific cytotoxic T-lymphocyte responses in HIV-infected Zambians. *J. Virol.* 71:8908-8911.
20. Cao, H., P. Kanki, J.L. Sankale, A. Dieng-Sarr, G.P. Mazzara, S.A. Kalams, B. Korber, S. Mboup, and B.D. Walker. 1997. Cytotoxic T-lymphocyte cross-reactivity among different human immunodeficiency virus type 1 clades: implications for vaccine development. *J. Virol.* 71:8615–8623.
21. Ferrari, G., W. Humphrey, M.J. McElrath, J.L. Excler, A.M. Duliege, M.L. Clements, L.C. Corey, D.P. Bolognesi, and K.J. Weinhold. 1997. Clade B-based HIV-1 vaccines elicit cross-clade cytotoxic T lymphocyte reactivities in uninfected volunteers. *Proc. Natl. Acad. Sci. USA.* 94:1396–1401.
22. McAdam, S., P. Kaleebu, P. Krausa, P. Goulder, N. French, B. Collin, T. Blanchard, J. Whitworth, A. McMichael, and F. Gotch. 1998. Cross-clade recognition of p55 by cytotoxic T lymphocytes in HIV-1 infection. *AIDS.* 12:571–579.
23. Buseyne, F., M.L. Chaix, B. Fleury, O. Manigard, M. Burgard, S. Blanche, C. Rouzioux, and Y. Riviere. 1998. Cross-clade-specific cytotoxic T lymphocytes in HIV-1-infected children. *Virology.* 250:316–324.
24. Graham, B.S. 2002. Clinical trials of HIV vaccines. *Annu. Rev. Med.* 53:207–221.
25. McMichael, A., and T. Hanke. 2002. The quest for an AIDS vaccine: is the CD8+ T-cell approach feasible? *Nat. Rev. Immunol.* 2:283–291.
26. Goulder, P.J., M.A. Altfeld, E.S. Rosenberg, T. Nguyen, Y. Tang, R.L. Eldridge, M.M. Addo, S. He, J.S. Mukherjee, M.N. Phillips, et al. 2001. Substantial differences in specificity of HIV-specific cytotoxic T cells in acute and chronic HIV infection. *J. Exp. Med.* 193:181–194.
27. Zhu, Y.Y., E.M. Machleder, A. Chenchik, R. Li, and P.D. Siebert. 2001. Reverse transcriptase template switching: a SMART approach for full-length cDNA library construction. *Biotechniques.* 30:892–897.
28. Douek, D.C., M.R. Betts, J.M. Brenchley, B.J. Hill, D.R. Ambrozak, K.L. Ngai, N.J. Karandikar, J.P. Casazza, and R.A. Koup. 2002. A novel approach to the analysis of specificity, clonality, and frequency of HIV-specific T cell responses reveals a potential mechanism for control of viral escape. *J. Immunol.* 168:3099–3104.
29. Garboczi, D.N., D.R. Madden, and D.C. Wiley. 1994. Five viral peptide-HLA-A2 co-crystals. Simultaneous space group determination and X-ray data collection. *J. Mol. Biol.* 239: 581–587.
30. Stewart-Jones, G.B., A.J. McMichael, J.I. Bell, D.I. Stuart, and E.Y. Jones. 2003. A structural basis for immunodominant human T cell receptor recognition. *Nat. Immunol.* 4:657–663.
31. Otwinowski, Z., and W. Minor. 1997. Processing of X-ray diffraction data collected in oscillation mode. *Methods Enzymol.* 276:307–326.
32. Kissinger, C.R., D.K. Gehlhaar, and D.B. Fogel. 1999. Rapid automated molecular replacement by evolutionary search. *Acta Crystallogr. D. Biol. Crystallogr.* 55:484–491.
33. Brunger, A.T., P.D. Adams, G.M. Clore, W.L. DeLano, P. Gros, R.W. Grosse-Kunstleve, J.S. Jiang, J. Kuszewski, M. Nilges, N.S. Pannu, et al. 1998. Crystallography & NMR system: a new software suite for macromolecular structure deter-

mination. *Acta Crystallogr. D. Biol. Crystallogr.* 54:905–921.
34. Jones, T.A., J.Y. Zou, S.W. Cowan, and Kjeldgaard. 1991. Improved methods for building protein models in electron density maps and the location of errors in these models. *Acta. Crystallogr. A.* 47:110–119.
35. Murshudov, G.N. 1997. Refinement of macromolecular structures by the maximum-likelihood method. *Acta Crystallogr. D. Biol. Crystallogr.* 53:240–255.
36. Perrakis, A., R. Morris, and V.S. Lamzin. 1999. Automated protein model building combined with iterative structure refinement. *Nat. Struct. Biol.* 6:458–463.
37. Stuart, D.I., M. Levine, H. Muirhead, and D.K. Stammers. 1979. Crystal structure of cat muscle pyruvate kinase at a resolution of 2.6 A. *J. Mol. Biol.* 134:109–142.
38. Esnouf, R.M. 1999. Further additions to MolScript version 1.4, including reading and contouring of electron-density maps. *Acta. Crystallogr. D. Biol. Crystallogr.* 55:938–940.
39. Cerundolo, V., J. Alexander, K. Anderson, C. Lamb, P. Cresswell, A. McMichael, F. Gotch, and A. Townsend. 1990. Presentation of viral antigen controlled by a gene in the major histocompatibility complex. *Nature.* 345:449–452.
40. van der Burg, S.H., M.R. Klein, C.J. van de Velde, W.M. Kast, F. Miedema, and C.J. Melief. 1995. Induction of a primary human cytotoxic T-lymphocyte response against a novel conserved epitope in a functional sequence of HIV-1 reverse transcriptase. *AIDS.* 9:121–127.
41. Willcox, B.E., G.F. Gao, J.R. Wyer, J.E. Ladbury, J.I. Bell, B.K. Jakobsen, and P.A. van der Merwe. 1999. TCR binding to peptide-MHC stabilizes a flexible recognition interface. *Immunity.* 10:357–365.
42. Yoo, S.H., and M.S. Lewis. 1995. Thermodynamic study of the pH-dependent interaction of chromogranin A with an intraluminal loop peptide of the inositol 1,4,5-trisphosphate receptor. *Biochemistry.* 34:632–638.
43. Atkins, P. 2001. Elements of Physical Chemistry. Oxford University Press, Oxford, England. 562 pp.
44. Sykulev, Y., M. Joo, I. Vturina, T.J. Tsomides, and H.N. Eisen. 1996. Evidence that a single peptide-MHC complex on a target cell can elicit a cytolytic T cell response. *Immunity.* 4:565–571.
45. Delon, J., C. Gregoire, B. Malissen, S. Darche, F. Lemaitre, P. Kourilsky, J.P. Abastado, and A. Trautmann. 1998. CD8 expression allows T cell signaling by monomeric peptide-MHC complexes. *Immunity.* 9:467–473.
46. Madden, D.R., D.N. Garboczi, and D.C. Wiley. 1993. The antigenic identity of peptide-MHC complexes: a comparison of the conformations of five viral peptides presented by HLA-A2. *Cell.* 75:693–708.
47. Sliz, P., O. Michielin, J.C. Cerottini, I. Luescher, P. Romero, M. Karplus, and D.C. Wiley. 2001. Crystal structures of two closely related but antigenically distinct HLA-A2/melanocyte-melanoma tumor-antigen peptide complexes. *J. Immunol.* 167:3276–3284.
48. Buslepp, J., R. Zhao, D. Donnini, D. Loftus, M. Saad, E. Appella, and E.J. Collins. 2001. T cell activity correlates with oligomeric peptide-major histocompatibility complex binding on T cell surface. *J. Biol. Chem.* 276:47320–47328.
49. Kuhns, J.J., M.A. Batalia, S. Yan, and E.J. Collins. 1999. Poor binding of a HER-2/neu epitope (GP2) to HLA-A2.1 is due to a lack of interactions with the center of the peptide. *J. Biol. Chem.* 274:36422–36427.
50. Reid, S.W., S. McAdam, K.J. Smith, P. Klenerman, C.A. O'Callaghan, K. Harlos, B.K. Jakobsen, A.J. McMichael, J.I. Bell, D.I. Stuart, and E.Y. Jones. 1996. Antagonist HIV-1 Gag peptides induce structural changes in HLA B8. *J. Exp. Med.* 184:2279–2286.
51. Garcia, K.C., M. Degano, R.L. Stanfield, A. Brunmark, M.R. Jackson, P.A. Peterson, L. Teyton, and I.A. Wilson. 1996. An alphabeta T cell receptor structure at 2.5 A and its orientation in the TCR-MHC complex. *Science.* 274:209–219.
52. Garboczi, D.N., P. Ghosh, U. Utz, Q.R. Fan, W.E. Biddison, and D.C. Wiley. 1996. Structure of the complex between human T-cell receptor, viral peptide and HLA-A2. *Nature.* 384:134–141.
53. Baker, B.M., Y.H. Ding, D.N. Garboczi, W.E. Biddison, and D.C. Wiley. 1999. Structural, biochemical, and biophysical studies of HLA-A2/altered peptide ligands binding to viral-peptide-specific human T-cell receptors. *Cold Spring Harb. Symp. Quant. Biol.* 64:235–241.
54. Rudolph, M.G., and I.A. Wilson. 2002. The specificity of TCR/pMHC interaction. *Curr. Opin. Immunol.* 14:52–65.
55. Reiser, J.B., C. Darnault, C. Gregoire, T. Mosser, G. Mazza, A. Kearney, P.A. van der Merwe, J.C. Fontecilla-Camps, D. Housset, and B. Malissen. 2003. CDR3 loop flexibility contributes to the degeneracy of TCR recognition. *Nat. Immunol.* 4:241–247.
56. Anikeeva, N., T. Lebedeva, M. Krogsgaard, S.Y. Tetin, E. Martinez-Hackert, S.A. Kalams, M.M. Davis, and Y. Sykulev. 2003. Distinct molecular mechanisms account for the specificity of two different T-cell receptors. *Biochemistry.* 42:4709–4716.
57. Goh, C.S., D. Milburn, and M. Gerstein. 2004. Conformational changes associated with protein-protein interactions. *Curr. Opin. Struct. Biol.* 14:104–109.
58. Savage, P.A., J.J. Boniface, and M.M. Davis. 1999. A kinetic basis for T cell receptor repertoire selection during an immune response. *Immunity.* 10:485–492.
59. van der Merwe, P.A., and S.J. Davis. 2003. Molecular interactions mediating T cell antigen recognition. *Annu. Rev. Immunol.* 21:659–684.
60. Wu, L.C., D.S. Tuot, D.S. Lyons, K.C. Garcia, and M.M. Davis. 2002. Two-step binding mechanism for T-cell receptor recognition of peptide MHC. *Nature.* 418:552–556.
61. Mason, D. 1998. A very high level of crossreactivity is an essential feature of the T-cell receptor. *Immunol. Today.* 19: 395–404.
62. Reiser, J.B., C. Darnault, A. Guimezanes, C. Gregoire, T. Mosser, A.M. Schmitt-Verhulst, J.C. Fontecilla-Camps, B. Malissen, D. Housset, and G. Mazza. 2000. Crystal structure of a T cell receptor bound to an allogeneic MHC molecule. *Nat. Immunol.* 1:291–297.
63. Moore, C.B., M. John, I.R. James, F.T. Christiansen, C.S. Witt, and S.A. Mallal. 2002. Evidence of HIV-1 adaptation to HLA-restricted immune responses at a population level. *Science.* 296:1439–1443.
64. Ding, Y.H., K.J. Smith, D.N. Garboczi, U. Utz, W.E. Biddison, and D.C. Wiley. 1998. Two human T cell receptors bind in a similar diagonal mode to the HLA-A2/Tax peptide complex using different TCR amino acids. *Immunity.* 8:403–411.
65. Ding, Y.H., B.M. Baker, D.N. Garboczi, W.E. Biddison, and D.C. Wiley. 1999. Four A6-TCR/peptide/HLA-A2 structures that generate very different T cell signals are nearly identical. *Immunity.* 11:45–56.
66. Schreiber, G., and A.R. Fersht. 1996. Rapid, electrostatically assisted association of proteins. *Nat. Struct. Biol.* 3:427–431.
67. Gakamsky, D.M., I.F. Luescher, and I. Pecht. 2004. T cell receptor-ligand interactions: a conformational preequilibrium or an induced fit. *Proc. Natl. Acad. Sci. USA.* 101:9063–9066.